

Effect of surface modification on the radiation stability of diamond ohmic contacts

Lian-Xi Mu(牟恋希), Shang-Man Zhao(赵上熳), Peng Wang(王鹏), Xiao-Lu Yuan(原晓芦), Jin-Long Liu(刘金龙), Zhi-Fu Zhu(朱志甫), Liang-Xian Chen(陈良贤), Jun-Jun Wei(魏俊俊), Xiao-Ping Ou-Yang(欧阳晓平), and Cheng-Ming Li(李成明)

Citation: Chin. Phys. B, 2024, 33 (**2**): 026801. DOI: 10.1088/1674-1056/ace61e
Journal homepage: http://cpb.iphy.ac.cn; http://iopscience.iop.org/cpb

What follows is a list of articles you may be interested in

Ohmic and Schottky contacts of hydrogenated and oxygenated boron-doped single-crystal diamond with hill-like polycrystalline grains

Jing-Cheng Wang(王旌丞), Hao Chen(陈浩), Lin-Feng Wan(万琳丰), Cao-Yuan Mu(牟草源), Yao-Feng Liu(刘尧峰), Shao-Heng Cheng(成绍恒), Qi-Liang Wang(王启亮), Liu-An Li(李柳暗), and Hong-Dong Li(李红东)
Chin. Phys. B, 2021, 30 (**9**): 096803. DOI: 10.1088/1674-1056/ac032b

First-principles study of high performance lithium/sodium storage of $Ti_3C_2T_2$ nanosheets as electrode materials

Li-Na Bai(白丽娜), Ling-Ying Kong(孔令莹), Jing Wen(温静), Ning Ma(马宁), Hong Gao(高红), Xi-Tian Zhang(张喜田)
Chin. Phys. B, 2020, 29 (**1**): 016802. DOI: 10.1088/1674-1056/ab592e

Electrical properties and microstructural characterization of Ni/Ta contacts to n-type 6H-SiC

Zhou Tian-Yu (周天宇), Liu Xue-Chao (刘学超), Huang Wei (黄维), Zhuo Shi-Yi (卓世异), Zheng Yan-Qing (郑燕青), Shi Er-Wei (施尔畏)
Chin. Phys. B, 2015, 24 (**12**): 126801. DOI: 10.1088/1674-1056/24/12/126801

Low contact resistivity between Ni/Au and p-GaN through thin heavily Mg-doped p-GaN and p-InGaN compound contact layer

Li Xiao-Jing (李晓静), Zhao De-Gang (赵德刚), Jiang De-Sheng (江德生), Chen Ping (陈平), Zhu Jian-Jun (朱建军), Liu Zong-Shun (刘宗顺), Le Ling-Cong (乐伶聪), Yang Jing (杨静), He Xiao-Guang (何晓光)
Chin. Phys. B, 2015, 24 (**11**): 116803. DOI: 10.1088/1674-1056/24/11/116803

Effects of annealing temperature on the electrical property and microstructure of aluminum contact on n-type 3C-SiC

Dai Chong-Chong (代冲冲), Liu Xue-Chao (刘学超), Zhou Tian-Yu (周天宇), Zhuo Shi-Yi (卓世异), Shi Biao (石彪), Shi Er-Wei (施尔畏)
Chin. Phys. B, 2014, 23 (**6**): 066803. DOI: 10.1088/1674-1056/23/6/066803

Effect of surface modification on the radiation stability of diamond ohmic contacts

Lian-Xi Mu(牟恋希)[1], Shang-Man Zhao(赵上熳)[1], Peng Wang(王鹏)[1], Xiao-Lu Yuan(原晓芦)[2], Jin-Long Liu(刘金龙)[1,†], Zhi-Fu Zhu(朱志甫)[3], Liang-Xian Chen(陈良贤)[1], Jun-Jun Wei(魏俊俊)[1], Xiao-Ping Ou-Yang(欧阳晓平)[4], and Cheng-Ming Li(李成明)[1,‡]

[1] *Institute for Advanced Materials and Technology, University of Science and Technology Beijing, Beijing* 100083, *China*
[2] *School of Mechanical Engineering, University of Science and Technology Beijing, Beijing* 100083, *China*
[3] *School of Information Engineering, Zhengzhou University of Technology, Zhengzhou* 450044, *China*
[4] *State Key Laboratory of Intense Pulsed Radiation Simulation and Effect, Northwest Institute of Nuclear Technology, Xi'an* 710024, *China*

(Received 13 May 2023; revised manuscript received 29 June 2023; accepted manuscript online 11 July 2023)

The ohmic contact interface between diamond and metal is essential for the application of diamond detectors. Surface modification can significantly affect the contact performance and eliminate the interface polarization effect. However, the radiation stability of a diamond detector is also sensitive to surface modification. In this work, the influence of surface modification technology on a diamond ohmic contact under high-energy radiation was investigated. Before radiation, the specific contact resistivities (ρ_c) between Ti/Pt/Au-hydrogen-terminated diamond (H-diamond) and Ti/Pt/Au-oxygen-terminated diamond (O-diamond) were 2.0×10^{-4} Ω·cm^2 and 4.3×10^{-3} Ω·cm^2, respectively. After 10 MeV electron radiation, the ρ_c of Ti/Pt/Au H-diamond and Ti/Pt/Au O-diamond were 5.3×10^{-3} Ω·cm^2 and 9.1×10^{-3} Ω·cm^2, respectively. The rates of change of ρ_c of H-diamond and O-diamond after radiation were 2550% and 112%, respectively. The electron radiation promotes bond reconstruction of the diamond surface, resulting in an increase in ρ_c.

Keywords: single crystal diamond, ohmic contact, surface modification, electron radiation

PACS: 68.47.Fg, 71.55.Cn, 73.40.Cg, 72.20.–i **DOI:** 10.1088/1674-1056/ace61e

1. Introduction

Diamond has many excellent properties, such as a high breakdown field, high carrier saturation velocity and high thermal conductivity, and is an ideal choice for next-generation semiconductor devices, especially in harsh environments. Diamond field-effect transistors have shown promising performance in high-power and high-frequency operations.[1,2] Diamond radiation detectors have also been used in large-scale scientific facilities, such as the radial neutron camera and HL-2A tokamak.[3,4] In addition, as the core component of solar-blind detection and imaging systems, solar-blind photodetectors have become a focus of research. Fast response to solar-blind ultraviolet is also one of the important applications of diamond detectors.[5,6]

Due to the chemical inertia of diamond, it is difficult to achieve strong interface bonding and a low barrier potential between the metal electrode material and diamond simultaneously. The electrons generated by radiation, under the action of the applied electric field, will accumulate charge in the crystal and build an internal electric field if the electrical contact is not able to extract and inject electrons fast enough. Therefore, the good electrical properties of diamond are unable to be fully exploited.[7] Surface modification and a diamond-like carbon layer have been used to optimize the diamond ohmic contact.[8–10] As the common terminations of diamond, hydrogen and oxygen (H-diamond and O-diamond) have demonstrated different surface properties. For instance, H-diamond shows a negative electron affinity (NEA) and surface conductivity, but under continuous low-energy electron irradiation, the secondary electron emission intensity of H-diamonds films is decayed.[11] O-diamond can be used as an excellent surface isolation and passivation layer. In addition, radiation stability is also important for device application. Diamond detectors were irradiated by proton beams with an energy of 4.5 MeV and the results indicated that with increase in the proton fluence the charge collection efficiency was decreased.[12] Ade *et al.*[13] studied the radiation resistance of high-pressure/high-temperature (HPHT) and chemical vapor deposited diamonds under 6 MeV–14 MeV electron therapy beams. The results showed that HPHT diamond had better stability of response to radiation.

During the preparation of a diamond radiation detector, the performance of the device is determined by the diamond material and interface. At present, research has mainly focused on the influence of radiation on device performance and the diamond material. However, the mechanism of the influence of high-energy radiation on the diamond ohmic contact has not been systematically studied. In order to further improve the performance of diamond detectors and re-

†Corresponding author. E-mail: liujinlong@ustb.edu.cn
‡Corresponding author. E-mail: chengmli@mater.ustb.edu.cn

© 2024 Chinese Physical Society and IOP Publishing Ltd

alize the application of diamond in electronic devices it is necessary to understand and control the influence of different terminal diamond surfaces on the contact resistance of the metal/semiconductor interface and the stability under high-energy irradiation. Due to a low contact resistance originating from an excellent affinity with carbon and relatively high diffusivity in diamond, after annealing Ti forms carbides with diamond. Heating above 425 °C caused transition from a rectifying to an ohmic contact. The ohmic property was retained during annealing at 750 °C for less than 60 min, even though Ti was diffused to the surface.[14]

In this study, H-diamond was prepared using HPHT diamond in a hydrogen plasma environment. O-diamond was obtained using HPHT diamond and heating in acid at high concentration. Based on the transmission line model (TLM), we researched the influence of surface modification technology on a diamond ohmic contact using typical electrode materials (Ti/Pt/Au) under high-energy radiation. Before radiation, the specific contact resistivities (ρ_c) of H-diamond and O-diamond were measured under the same conditions. After high-energy electron radiation of 10 MeV, ρ_c was measured and the interface resistance between H-diamond and O-diamond was analyzed.

2. Experiment

A schematic diagram of the process for preparing diamond ohmic contacts for H-diamond and O-diamond is shown in Fig. 1. Two Ib type HPHT single-crystal (100) diamonds with a size of 4 mm × 4 mm were used in this experiment. The substrates were fine polished to obtain a relatively flat surface. The pressure and time were 550 Pa and 10 min, respectively, and the surface roughness was less than 1 nm. After polishing, the samples were boiled in acidic solution (HNO_3:H_2SO_4 = 1:3 by volume) for 30 min and ultrasonically cleaned in acetone, alcohol and deionized water sequentially for 15 min to obtain O-diamond and remove the non-diamond impurities. The H-diamond epitaxial layer was prepared based on the O-diamond in a self-made microwave plasma chemical vapor deposition (MPCVD) system. The cavity pressure, microwave power, H_2 flow rate, CH_4 flow rate and time were 9.1 kPa, 1300 W, 300 sccm, 0.9 sccm and 30 min, respectively.

By photolithographic technology, an area of 100 μm × 100 μm with unequal spacing was patterned on H-diamond and O-diamond. Ti (10 nm)/Pt (20 nm)/Au (100 nm) were prepared by electron beam evaporation on both H-diamond and O-diamond. After the electrode was plated, the H-diamond and O-diamond were annealed at 680 °C for 30 min under hydrogen plasma to form a conductive channel and ohmic contact. The 10 MeV electron beam irradiation experiment was conducted on a linear electron accelerator. The electron flux was 3×10^{12} electrons·cm^{-2}·s^{-1} and the irradiation time was 10 s. After irradiation, the *I*–*V* characteristics of the samples were measured.

The *I*–*V* characteristics were measured with an Agilent B1500 A parameter analyzer. The quality of diamond crystal was measured by high spectral resolution analytical grade confocal Raman microscope (inVia Qontor) with a laser wavelength of 532 nm and focus spot size of 40 μm. The integration time interval was 10 s, the Raman shift range was 800 cm^{-1}–2000 cm^{-1}, the microscopic size range was ≥ 1 μm and the spectral resolution was 1 cm^{-1}. A contact angle measuring instrument (DSA100) was used to characterize the wettability of H-diamond and O-diamond surfaces.

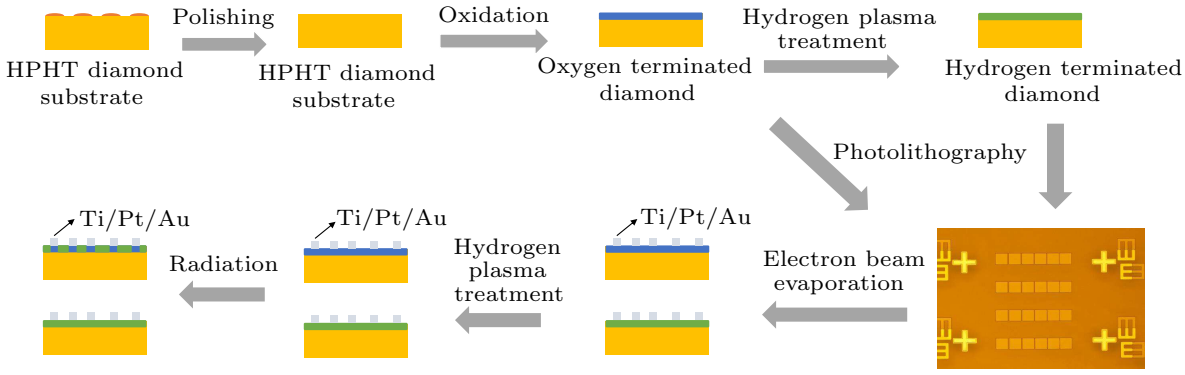


Fig. 1. Schematic diagram of the process for preparing diamond ohmic contacts for H-diamond and O-diamond.

3. Result and discussion

The Raman spectroscopy characterization results using a 532 nm laser are shown in Fig. 2. The Raman characteristic peaks and their full width at half maximum of H-diamond and O-diamond were 1332.53 cm^{-1} and 1332.61 cm^{-1} and 6.77 cm^{-1} and 6.75 cm^{-1}, respectively. The stress (*P*) in the diamond samples can be expressed as $P = \Delta\nu/k$, where $\Delta\nu$ is the displacement of the Raman characteristic peak of single-crystal diamond relative to the unstressed Raman peak and k is the Raman stress factor of diamond, which has been measured as 1.9 cm^{-1}·GPa^{-1}. The Raman displacement of natural synthetic diamond at room temperature is

1332.3 ± 0.2 cm^{-1}.[15] In this study, P in the H-diamond and O-diamond was -0.12 GPa and -0.16 GPa, respectively. The D peak (1350 cm^{-1}) and G peak (1580 cm^{-1}) of the disordered carbon and graphite were not observed in the Raman spectrum.[16]

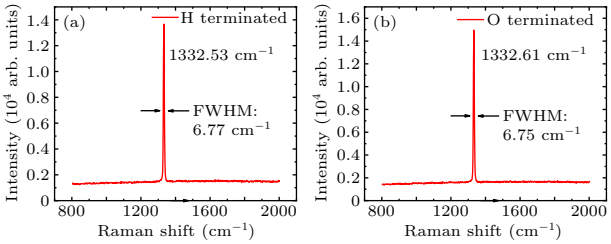


Fig. 2. Laser Raman spectra of (a) H-diamond and (b) O-diamond at 532 nm excitation.

The surface properties of H-diamond and O-diamond were studied with a contact angle measuring instrument. The contact angles of deionized water on H-diamond and O-diamond were 91.5° and 52.5°, respectively. Wetting theory shows that for the same external adsorption medium, the smaller the surface energy of the solid surface the larger the contact angle, which shows hydrophobicity. Ostrovskaya *et al.*[17] obtained the surface free energies of H-diamond and O-diamond as 47 mJ·m^{-2} and 65.8 mJ·m^{-2}, respectively. O-diamond was achieved by introducing oxygen-containing functional groups such as C–O, C=O and –COOH, on the surface.[18] H-diamond was prepared under hydrogen plasma treatment after heating with strong oxidizing acids. The corresponding dangling bonds are occupied by hydrogen atoms or hydrogen molecules. The hydrocarbon groups induced by the hydrogen plasma treatment reduce the surface free energy and lead to hydrophobicity of the diamond surface. The surface area of H-diamond mainly comprises hydrogen functional groups such as C–H.[19] The main reason for the large difference between the contact angles of H-diamond O-diamond is that the different surface adsorption groups cause surface reconstruction, giving different surface free energies.

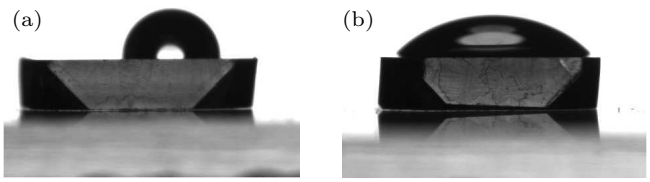


Fig. 3. Contact angle test: (a) H-diamond and (b) O-diamond.

After annealing at 680 °C, the I–V characteristic curves of H-diamond and O-diamond were measured. Ohmic contacts were formed with different spaces. The spaces designed in the photolithographic mask were 2 μm, 4 μm, 6 μm, 8 μm and 10 μm, and the rectangle size was 100 μm^2 after metal plating due to accurate photolithography. For H-diamond, the spaces between adjacent rectangles were remeasured under the optical microscope as 3.8 μm, 5.3 μm, 7.0 μm, 9.1 μm and 11.4 μm, respectively, and the rectangle size was 100 μm^2. The spaces between adjacent rectangles of O-diamond were 10.6 μm, 12.4 μm, 14.8 μm and 15.7 μm, respectively, and the rectangle size was 100 μm^2. For TLM measurement, the total resistance $R_{\rm tot}$ (obtained from V/I) for a rectangular geometry can be expressed as[20,21]

$$R_{\rm tot}(l) = 2R_{\rm c} + \frac{R_{\rm s}}{W} \times l, \tag{1}$$

$$\rho_{\rm c} = (R_{\rm c}^2 \cdot W^2)/R_{\rm s}, \tag{2}$$

where $R_{\rm c}$ denotes the total contact resistance, $R_{\rm s}$ is the semiconductor thin layer resistance between ohmic contacts, l is the space between rectangles, W is the width of the contact pad and $\rho_{\rm c}$ is specific contact resistivity. When $R_{\rm tot}$ is plotted as a linear function of l, $\rho_{\rm c}$ can be calculated according to Eq. (2). In Figs. 4(a) and 4(c), the I–V measurements are exhibited as functions of the space between two adjacent pads of the TLM pattern. It can be clearly seen that both H-diamond and O-diamond contacts have a linear I–V characteristic and the $R_{\rm tot}$ between any two adjacent contact pads can be deduced. $R_{\rm tot}$ between the pairs of contacts versus the contact spacing l for H-diamond and O-diamond annealed at 680 °C is shown in Figs. 4(b) and 4(d), and the $\rho_{\rm c}$ values are calculated to be 2.0×10^{-4} Ω·cm^2 and 4.3×10^{-3} Ω·cm^2, respectively, according to Eq. (2). The $\rho_{\rm c}$ value is comparable to Chen's report,[22] in which the specific $\rho_{\rm c}$ value of boron-doped diamond and a Ti/Pt/Au metal electrode was 10^{-4} Ω·cm^2.

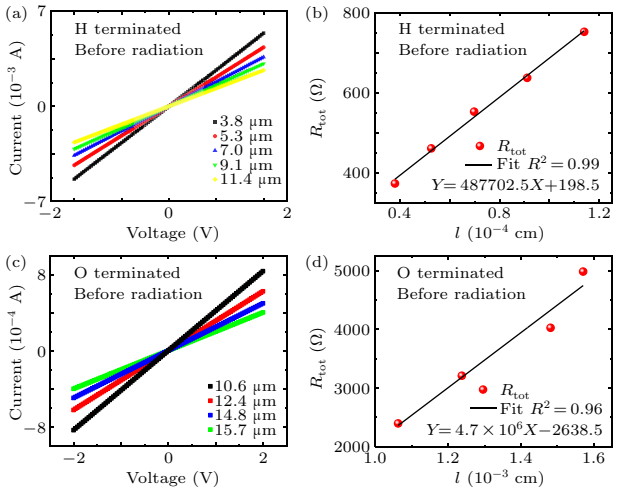


Fig. 4. TLM I–V characteristics of (a) H-diamond and (c) O-diamond with different spacings between two adjacent patterns, before radiation. Dependence of $R_{\rm tot}$ on l for (b) H-diamond and (d) O-diamond.

In order to test the stability of H-diamond and O-diamond, 10 MeV electron beam irradiation experiments were carried out in a linear electron accelerator. The electron flux was 3×10^{12} electrons·cm^{-2}·s^{-1} and the irradiation time was 10 s. After irradiation, the I–V characteristic curves of the samples were tested. As shown in Figs. 5(a) and 5(c), the I–V

characteristic curves of H-diamond and O-diamond are linear, forming an ohmic contact. As shown in Figs. 5(b) and 5(d), by calculation the ρ_c values for H-diamond and O-diamond after radiation are 5.3×10^{-3} Ω·cm^2 and 9.1×10^{-3} Ω·cm^2, respectively. Figure 6 summarizes the change in ρ_c of H-diamond and O-diamond before and after irradiation.

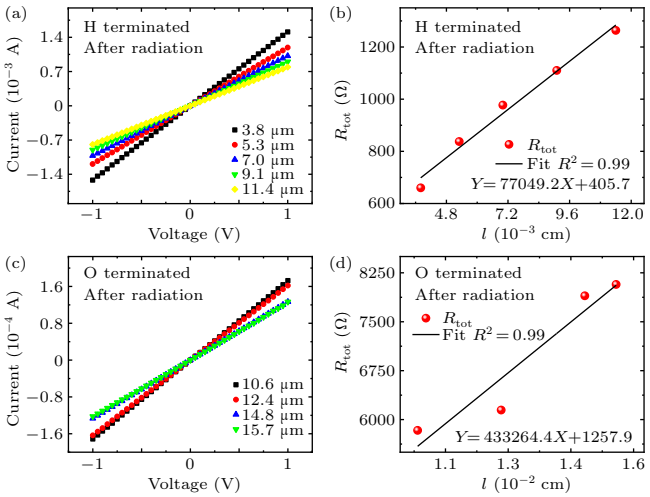


Fig. 5. TLM *I*–*V* characteristics of (a) H-diamond and (c) O-diamond with different spacing between two adjacent patterns, after radiation. Dependence of R_{tot} on l for (b) H-diamond and (d) O-diamond.

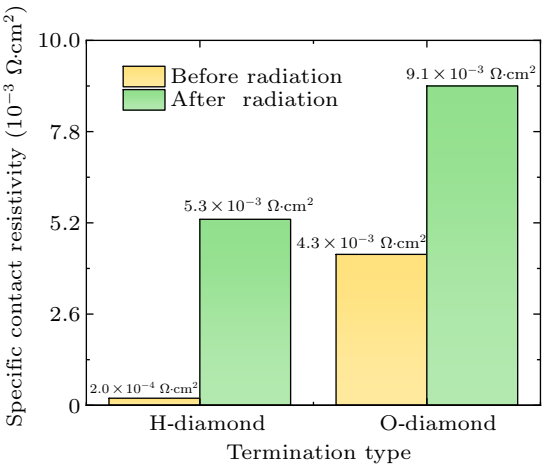


Fig. 6. Specific contact resistivity before and after irradiation of H-diamond and O-diamond.

A schematic diagram of the diamond interface before and after irradiation is shown in Fig. 7. Exposure of the surface of H-diamond to air leads to the generation of surface conductance. The surface conductive channel of H-diamond is located at 10 nm–30 nm below the surface, exhibiting conductivity characteristics similar to a two-dimensional hole gas.[23,24] This model suggests that the adsorption of materials with low unoccupied electron states on the surface of H-diamond is a sufficient condition for surface conductivity. In order to accumulate enough holes in the subsurface region of the diamond when hydrogen acts as an impurity level, valence band electrons can be realized by transiting to the adsorption layer of the low unoccupied energy state, and a doping effect is achieved by electron transfer.[25] Therefore, H-diamond shows p-type conductivity and has a NEA. The work function of the surface of H-diamond exposed to air is about 5.3 eV.[26] The electron affinity of (100) H-diamond is −1.3 eV to −0.4 eV.[27,28] O-diamond has a positron affinity of 1.7 eV.[29] Zhang *et al.*[30] demonstrated that O-diamond can efficiently pin the Fermi level in a fixed position regardless of the metallic material. Because H-diamond has NEA it is conducive to electron transmission when forming an ohmic contact. The *I*–*V* curve measurement results show that R_{tot} and ρ_c of H-diamond are lower than those of O-diamond. H-diamond can reduce the resistance and improve ohmic contact. After 10 MeV electron radiation, R_{tot} and ρ_c of H-diamond and O-diamond increased. The rates of change of ρ_c of H-diamond and O-diamond after radiation were 2550% and 112%, respectively. The reason for the increase in contact resistance is explained below. Generally, an O-termination is more stable than an H-termination on the diamond surface. Foord *et al.*[31] observed that the uptake of oxygen on O-diamond was slower than on H-diamond, and an explanation for the enhanced reactivity could be that the hydrogenation used here essentially roughened the surface, thus leading to more surface sites on which oxygen could adsorb. For the H-terminated diamond, 10 MeV electron radiation would promote the formation of C=O bonds, reducing the number of C–H bonds on the surface.[32] Meanwhile, electron beam bombardment destroys the H-diamond and decreases the film's NEA, resulting in substantial degradation of surface conductivity.[33] After irradiation, the C=O bonds were enhanced, which is the main reason for the increase in contact resistance of O-terminated diamond.[32] The increase in interface resistance caused by radiation may also be an important factor leading to degradation of the performance of diamond detectors.

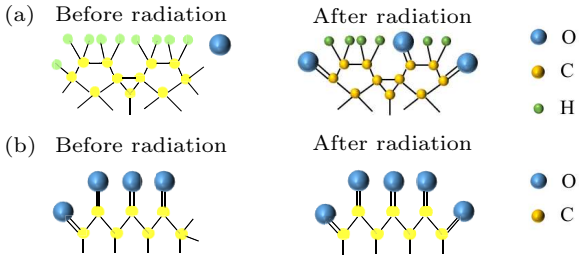


Fig. 7. Schematic diagram of the diamond interface before and after radiation: (a) H-diamond and (b) O-diamond.

4. Conclusion

In this work, based on the TLM, the influence of surface modification technology on diamond ohmic contacts was researched. After annealing, the specific contact resistivities of H-terminated diamond–Ti/Pt/Au and O-terminated diamond–Ti/Pt/Au were 2.0×10^{-4} Ω· cm^2 and 4.3×10^{-3} Ω·cm^2, respectively. After 10 MeV electron radiation, the specific contact resistivities of H-terminated diamond and O-terminated

diamond were 5.3×10^{-3} Ω·cm^2 and 9.1×10^{-3} Ω·cm^2, respectively. After radiation, the rates of change of specific contact resistivity of H-terminated diamond and O-terminated diamond were 2550% and 112%, respectively. By contrast, H-terminated diamond showed lower resistivity, while the surface of O-terminated diamond was relatively stable.

Acknowledgment

Project supported by the National Key Research and Development Program of China (Grant No. 2022YFB3608601).

References

[1] Verona C, Ciccognani W, Colangeli S, Limiti E, Marinelli M, Santoni E, Verona-Rinati G, Angelone M, Pillon M, Pompili F, Benetti M, Cannata D and Di Pietrantonio F 2016 *IEEE Electron Dev. Lett.* **37** 1597

[2] Yamaguchi T, Umezawa H, Ohmagari S, Koizumi H and Kaneko JH 2021 *Appl. Phys. Lett.* **118** 162105

[3] Esposito B, Marocco D, Gandolfo G, *et al.* 2022 *J. Fusion Energy* **41** 22

[4] Qu Y F, Zang L G, Chen W, Hou Y M, Lu J and Luo Y 2022 *Rev. Sci. Instrum.* **93** 113507

[5] Zhang Z F, Lin C N, Yang X, Tian Y Z, Gao C J, Li K Y, Zang J H, Yang X G, Dong L and Shan C X 2021 *Carbon* **173** 427

[6] Girolami M, Serpente V, Mastellone M, Tardocchi M, Rebai M, Xiu, Q L, Liu J L, Sun Z J, Zhao Y B, Valentini V and Trucchi D M 2022 *Carbon* **189** 27

[7] Galbiati A, Lynn S, Oliver K, Schirru F, Nowak T, Marczewska B, Duenas J A, Berjillos R, Martel I and Lavergne L 2009 *IEEE Transactions on Nuclear Science* **56** 1863

[8] Wang J C, Chen H, Wan L F, Mu C Y, Liu Y F, Cheng S H, Wang Q D, Li A L and Li H D 2021 *Chin. Phys. B* **30** 096803

[9] Su K, Pen Z Y, Zhang J F, Liu L Y, Zhang J C, Zhang Y C, He Q, Zhang C F, Ouyang X P and Hao Y 2020 *Appl. Phys. Lett.* **116** 092104

[10] Okhapkin A I, Yunin P A, Arkhipova E A, Kraev S A, Korolyov S A, Drozdov M N and Shashkin V I 2020 *Semiconductors* **54** 1056

[11] Hoffman A, Laikhtman A, Ustaze S, Hamou M H, Hedhili M N, Guillotin J P, Le Coat Y and Azria R 2002 *J. Appl. Phys.* **91** 4726

[12] Grilj V, Skukan N, Jaksic M, Pomorski M, Kada W, Kamiya T and Ohshima T 2016 *Nucl. Instrum. Meth. B* **372** 161

[13] Ade N, Nam T L, Derry T E and Mhlanga S H 2014 *Radiat. Phys. Chem.* **98** 155

[14] Hoshino Y, Saito Y and Nakata J 2010 *J. Appl. Phys.* **49** 101302

[15] Bergman L and Nemanich R J 1995 *J. Appl. Phys.* **78** 6709

[16] Lee E H, Hembree D M, Rao G R and Mansur L K 1993 *Phys. Rev. B* **48** 15540

[17] Ostrovskaya L, Perevertailo V, Ralchenko V, Dementjev A and Loginova O 2002 *Diam. Relat. Mater.* **11** 845

[18] Tu J L, Shi J D, Chen L X, Liu J L, Li C M and Wei J J 2022 *Int. J. Heat Mass Transfer* **199** 123481

[19] Kawarada H 1996 *Surf. Sci. Rep.* **26** 205

[20] Berger H H 1972 *Solid-State Electronics* **15** 145

[21] Zhao D, Li F N, Liu Z C, Chen X D, Wang Y F, Shao G Q, Zhu T F, Zhang M H, Zhang J W, Wang J J, Wang W and Wang H X 2018 *Appl. Surf. Sci.* **443** 361

[22] Chen Y G, Ogura A, Yamasaki S and Okushi H 2004 *Diam. Relat. Mater.* **13** 2121

[23] Hirama K, Takayanagi H, Yamauchi S, Yang J H, Kawarada H and Umezawa H 2008 *Appl. Phys. Lett.* **92** 112107

[24] Sauerer C, Ertl F, Nebel C E, Stutzmann M, Bergonzo P, Williams O A and Jackman R A 2001 *Phys. Status Solidi A* **186** 241

[25] Strobel P, Riedel M, Ristein J and Ley L 2004 *Nature* **430** 439

[26] Edmonds M T, Pakes C I, Mammadov S, Zhang W, Tadich A, Ristein J and Ley L 2011 *Phys. Status Solidi A* **208** 2062

[27] Maier F, Riedel M, Ristein J and Ley L 2001 *Diam. Relat. Mater.* **10** 506

[28] Kono S, Saitou T, Kawata H, Goto T, Kakefuda Y and Komeda T 2009 *Surf. Sci.* **603** 860

[29] Maier F, Ristein J and Ley L 2001 *Phys. Rev. B* **64** 165411

[30] Zhang S, Liu K, Liu B J, Zhang X H, Qiao P F, Zhao J W, Li Y C, Hao X B, Liang Y, Liang B, Zhang W C, Dai B, Han J C and Zhu J Q 2023 *Carbon* **205** 69

[31] Foord J S, Hian L C and Jackman R B 2001 *Diam. Relat. Mater.* **10** 710

[32] Bai M J, Liu J L, Jiang H, Li W J, Wei J J, Chen L X, Miao J Y and Li C M 2022 *Tribol. Int.* **176** 107910

[33] Wei K T, Li J, Liu B Y, Wu R R, Wei Q, Wu S L, Hu W B and Wang H X 2019 *Vacuum* **172** 109046